

# Segmented Circular Strip Planar Leaky-Wave Antenna Designs for Broadside Radiation and One-Sided Beam Scanning

Symon K. Podilchak<sup>1,2</sup>, Al P. Freundorfer<sup>2</sup>, Yahia M. M. Antar<sup>\*1</sup>

<sup>1</sup> Royal Military College of Canada, PO Box 17000, Station Forces, Kingston, Ontario Canada, K7K 7B4 (antar-y@rmc.ca)

<sup>2</sup> Queen's University, Kingston Ontario Canada, K7L 3N6

**ABSTRACT:** Planar antenna designs that utilize surface waves (SWs) for leaky wave (LW) excitation are investigated for millimeter wave frequencies of operation. Surface-wave launchers (SWLs) are employed as the antenna source generating cylindrical SWs for bound propagation on a grounded dielectric slab (GDS). By the addition of a segmented circular strip grating configuration, a partially reflecting surface (PRS) can be realized, providing suitable conditions for 2-D leaky-wave radiation. Directive pencil beam patterns at broadside, with gain values greater than 12 dBi at 19.5 GHz, can be achieved.

## INTRODUCTION

High gain planar leaky-wave antennas (LWAs) are attractive due to their low cost, ease of fabrication and compatibility with other devices and monolithic technologies. In general, these types of antennas consist of a planar guiding structure that can support the propagation of cylindrical leaky wave (LWs) on its guiding surface. Such cylindrical waves leak energy into free space during their radial propagation along the 2-D antenna aperture. With appropriate design these planar antennas can achieve directive radiation at broadside and pencil beam patterns that can scan as a function of frequency [1]-[6].

Recently printed Yagi-Uda like slot configurations have been recognized as a practical and efficient feeding technique for such 2-D planar LWAs [4]-[6]. In these designs a bound  $TM_0$  surface-wave (SW) mode is excited and unidirectional SW propagation occurs along the air dielectric interface. In [4] results of a broadside radiating segmented circular strip LWA were presented. Surface waves were launched onto a grounded dielectric slab (GDS) from a directive surface-wave launcher (SWL) source, and by the addition of a segmented circular strip grating, LWs were excited as illustrated in Fig. 1. In that paper measurements illustrated maximum gain at broadside ( $\theta_p = 0^\circ$ ) at 19.48 GHz. This work provides further insight into such LWAs by investigating the beam scanning capability as a function of frequency. Thus the increased functionality of the planar antenna is highlighted along with the associated radiation efficiencies. In addition, other designs are investigated by designing different strip gratings and results are compared by varying the directive SWL source configuration. Gain performances are examined as a function of frequency and beam angle. Results are shown in Figs. 2-5 and suggest that the segmented circular strip grating, frequency of operation, substrate properties and SWL source are all central in achieving maximum radiation at broadside.

## SEGMENTED CIRCULAR STRIP GRATINGS

Such an arrayed configuration of feedless strips can leak or radiate energy into free space with decreasing amplitude away from the SWL source [3], [4]. The magnetic field component of the cylindrical  $TM$  SW mode propagating along the guiding surface (from the SWL source placed at the origin) inductively couples to the strip segments with decreasing amplitude along the aperture. Leakage occurs along the guiding surface, thus defining LW radiation away from the 2-D planar antenna structure. Essentially, suitable boundary conditions are employed for strip resonance at the  $TE_1$  SW mode cutoff frequency of the utilized GDS ( $\epsilon_r = 10.2$ ,  $h = 1.27$  mm and  $\tan \delta = 0.0023$ ) ensuring radiation of both  $TM$  and  $TE$  field distributions, as required for broadside radiation from 2-D LWAs [3].

The four fabricated segmented circular strip grating configurations investigated in this work are shown in Fig. 2. The radius,  $\rho(m)$ , of each segmented concentric ring,  $m$ , can be defined by  $\rho(m) = \rho_0 + p_\rho(m - 1)$  where  $\rho_0 = 10$  mm and  $p_\rho = 7$  mm. The periodicity of each segment in the  $\hat{\phi}$  direction ( $p_\phi$ ) is 14 mm.

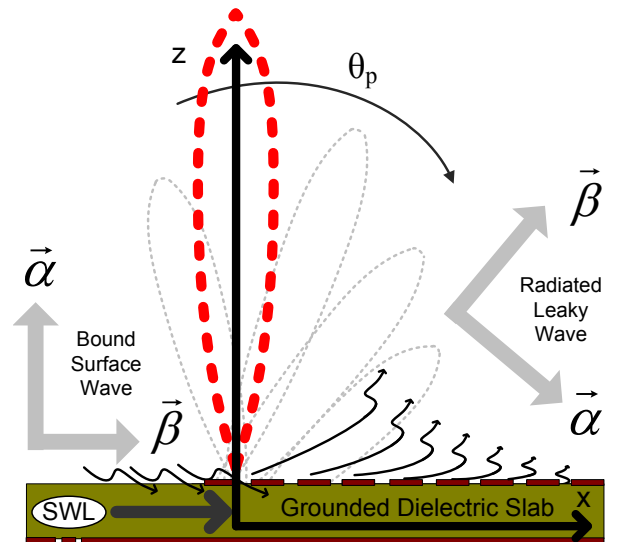


Figure 1: The slots embedded within the ground plane act as magnetic dipole sources for the investigated LWA structures. By the addition of a segmented circular strip grating, LWs can be excited offering broadside pencil beam patterns and conical-sector beam scanning in the far-field as a function of frequency. E ( $x$ - $z$ ) Plane shown referenced to the main slot of the SWL source.

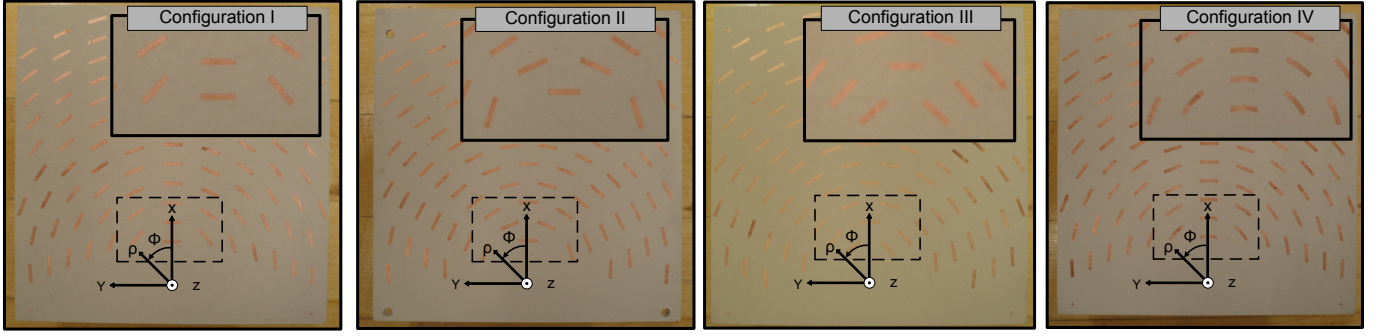


Figure 2: Fabricated and measured LWAs. Configuration I achieved maximum gain at broadside ( $\theta_p = 0^\circ$ ) while Configuration II-IV achieved gain maximums near broadside and in the forward direction ( $\theta_p \geq +3^\circ$ ). Configuration IV maintained the same strip placement and strip location as in Configuration I but with curved strips versus straight strips (the curvature of the strips were proportional to the radial position from the origin).

Configuration I was originally presented in [4] while the other LWA designs, Configurations II and III, were newly designed for this work by varying the strip placement in each ring while maintaining the  $\rho$  and  $\phi$  periodicities. As observed in Fig. 2, Configuration I has strips placed along the  $\hat{x}$ -axis for each ring segment. Conversely, Configuration II alters such placement every second ring while Configuration III is its inverse; i.e. the negative formation of Configuration II. Furthermore, Configuration I [II] [III] has 1 [1] [2] strip(s) in the first ring, 3 [4] [3] strips in the second ring and 5 [5] [6] strips in the third ring, and so on, as shown in Fig. 2.

For LWA Configurations I-III the realized rectangular strip lengths and widths were maintained at 7.25 mm and 1.25 mm, respectively. Conversely, Configuration IV was designed by curving each strip segment (curvature defined by the radius  $\rho(m)$  and the standard strip arc length of 7.25 mm) while maintaining strip position as in Configuration I. Utilized SWL source configurations are presented in Fig. 3 while far-field beam pattern measurements are presented in Figs. 4 and 5. Measured and simulated results illustrate that Configuration I achieves maximum gain values for near broadside beam angles ( $\theta_p = 0^\circ$ ).

## DIRECTIVE-FOLDED AND DIRECTIVE-UNFOLDED SURFACE-WAVE LAUNCHERS

The utilized planar antenna sources and simulated TM and TE field distributions are shown in Fig. 3. Essentially, the slotted configurations can act as magnetic dipole sources for the investigated LWA designs. The main radiating slot of the SWLs excites a cylindrical TM SW field distribution and unidirectional SW propagation is achieved by the addition of the secondary folded and unfolded reflector slots. In addition, the SWLs were fed by a coplanar waveguide transmission line allowing for simple integration with other monolithic technologies, planar circuit topologies and additional MMIC components.

Simulated TM and TE field distributions generated by the SWL sources (with no strips placed on top of the slab and with 1 Watt of power for port excitation) can be observed at 24 GHz and 0.5 mm above the air-dielectric interface. As shown in Figs. 3(b) and (e) the majority of the TM SW power (generated by the main slot) propagates in the forward  $x$  direction achieving unidirectional SW propagation. A TE field distribution is also observed in the  $\pm y$  directions (generated by the secondary slot segments [4]) as shown in Figs. 3(c) and (f). Reduced TE field strength levels are observed with directive-unfolded SWL as shown in Fig. 3(f). For instance, for  $(x, y) \in [0, \pm 5]$  mm TE field strength values are below 2000 [1400] V/m for the directive-folded [directive-unfolded] SWL.

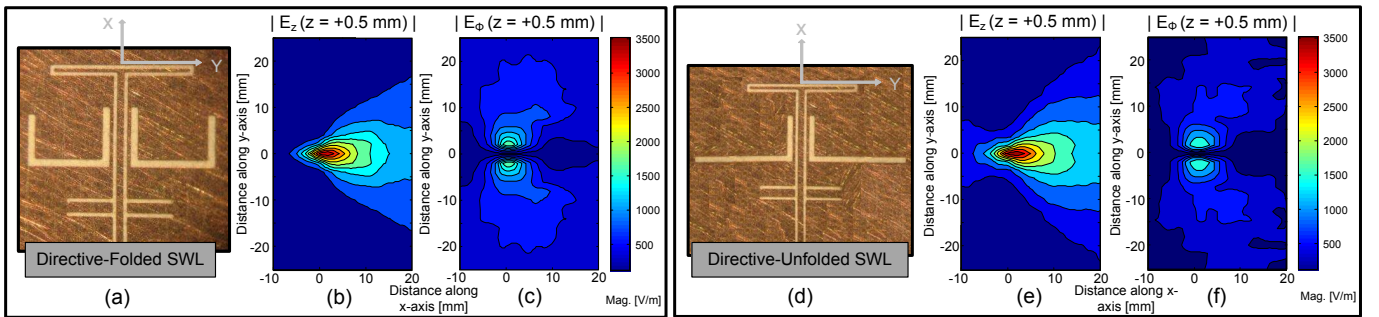


Figure 3: The folded and unfolded SWLs and the  $|E_z(x, y)|$  and  $|E_\phi(x, y)|$  field distributions 0.5 mm away from the air-dielectric interface at 24 GHz.

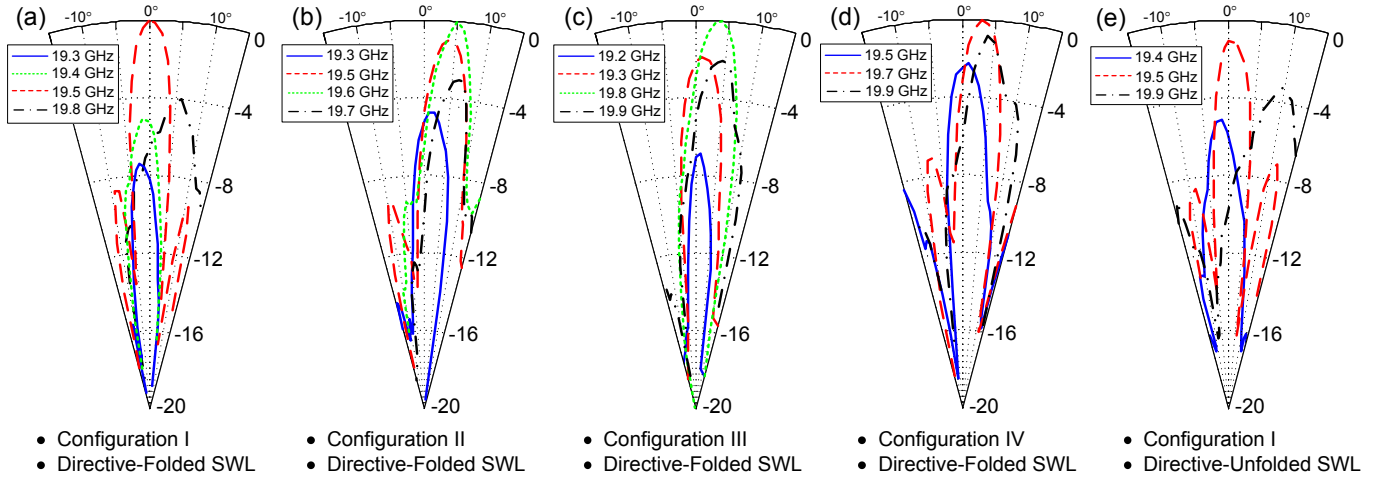


Figure 4: Measured far-field gain patterns shown in the  $E(x-z)$  plane for the investigated planar LWAs and noted SWL sources. Results are normalized to observed maximum for each Configuration (a-d). Reduced gain values (1.2 dB) at broadside (e) are observed for Configuration I using the directive-unfolded SWL source (when compared to the directive-folded SWL) due to reduced TE SW field excitations above the guiding surface as shown in Fig. 3.

In addition, by unfolding the secondary slots toward the  $\pm y$  directions increased TM field strengths can be observed (Fig. 3(e)) along the guiding surface due to the increase (by 45%) in secondary slot length. It should be noted that both TM and TE SW field configurations are required for broadside radiation and thus their excitation is desired for increased gain values at broadside. More specifically, for the realization of directive radiation at broadside both TM and TE radiated components,  $E_\theta$  and  $E_\phi$ , should combine and be approximately equal in both the  $E$  and  $H$  planes in the far-field [3], [4]. The directive-unfolded SWL achieves a larger effective aperture on the guiding surface (defined by the SW field distributions) but with reduced TE SW field excitations along the  $\hat{y}$ -axis and increased TM SW power directed in the backward  $-x$  direction (when compared to the directive-folded SWL). Thus reduced gain patterns at broadside are expected with the directive-unfolded SWL source configuration (when compared to the folded secondary slot source) due to the observed reduction in TE field strength.

## RESULTS AND DISCUSSION

Measurements for LWA Configuration I with a directive-folded SWL source are shown in Fig. 4(a). A main pencil beam with maximum gain can be observed at broadside ( $\theta_p = 0^\circ$ ) at 19.5 GHz just after the  $TE_1$  SW mode cutoff frequency (19.47 GHz) of the slab suggesting maximum radiation at the edge of a TE LW stopband [4]. In addition, these results also imply that both TM and TE cylindrical LWs were excited on the aperture and that the radiated far-field components,  $E_\theta$  and  $E_\phi$ , combined at broadside with approximately equal value in both principal planes [3], [4]. Gain values of 12.3 dBi can be observed at broadside.

In addition, one-sided beam scanning to the left of broadside ( $\theta_p = -3^\circ$ ), at broadside ( $\theta_p = 0^\circ$ ), and to the right of broadside ( $\theta_p = +5^\circ$ ) is observed as a function of frequency at 19.3, 19.5 and 19.8 GHz, respectively (with maximum gain observed at broadside). With a further increase in frequency the main pencil beam continues to scan towards end-fire and conical-sector beam scanning is observed as shown in Fig. 5. Essentially a progressive phase shift in current can be achieved on the radial strip aperture (due to the cylindrical SW phase front that couples power to the strip elements) generating the observed one-sided far-field beam patterns that scan as a function of frequency in the forward ( $\theta_p > 0^\circ$ ) direction.

It should be noted that diminished gain values (reduction of at worst 4 dB) are observed from 19.8 GHz to 20.1 GHz while an increase in gain at 20.32 GHz (by 0.73 dB) is observed for the conical-sector beam pattern at  $f = 20.32$  GHz (when compared to the broadside beam at 19.5 GHz). Similar pencil beam patterns and scanning behavior is observed for Configuration I using the directive-unfolded SWL source, but with reduced gain values (as shown in Fig. 4(e)) due to the reduced TE SW field strength (as illustrated in Fig. 3(f)).

Maximum radiation at broadside was not observed with Configurations II-IV as shown in Figs. 4 (b), (c) and (d), respectively. For all three designs maximum gain values are observed for  $\theta_p > 0^\circ$  in the forward direction. More specifically, beam maximums are observed at  $\theta_p = 5^\circ$  [4°] (3°) for Configuration I [III] (IV). Strong SW excitations may have caused an out of phase resonance response and the negative effects, due to mutual coupling between strip elements, may have been problematic explaining the reduced radiation performances at broadside. Moreover, a significant portion of the input the SW power may have been trapped as a bound mode and not radiated [7]. These results suggest LW stopband behavior at broadside for Configurations I-III and thus implying that proper segmented circular strip design is important in achieving maximum gain at broadside.

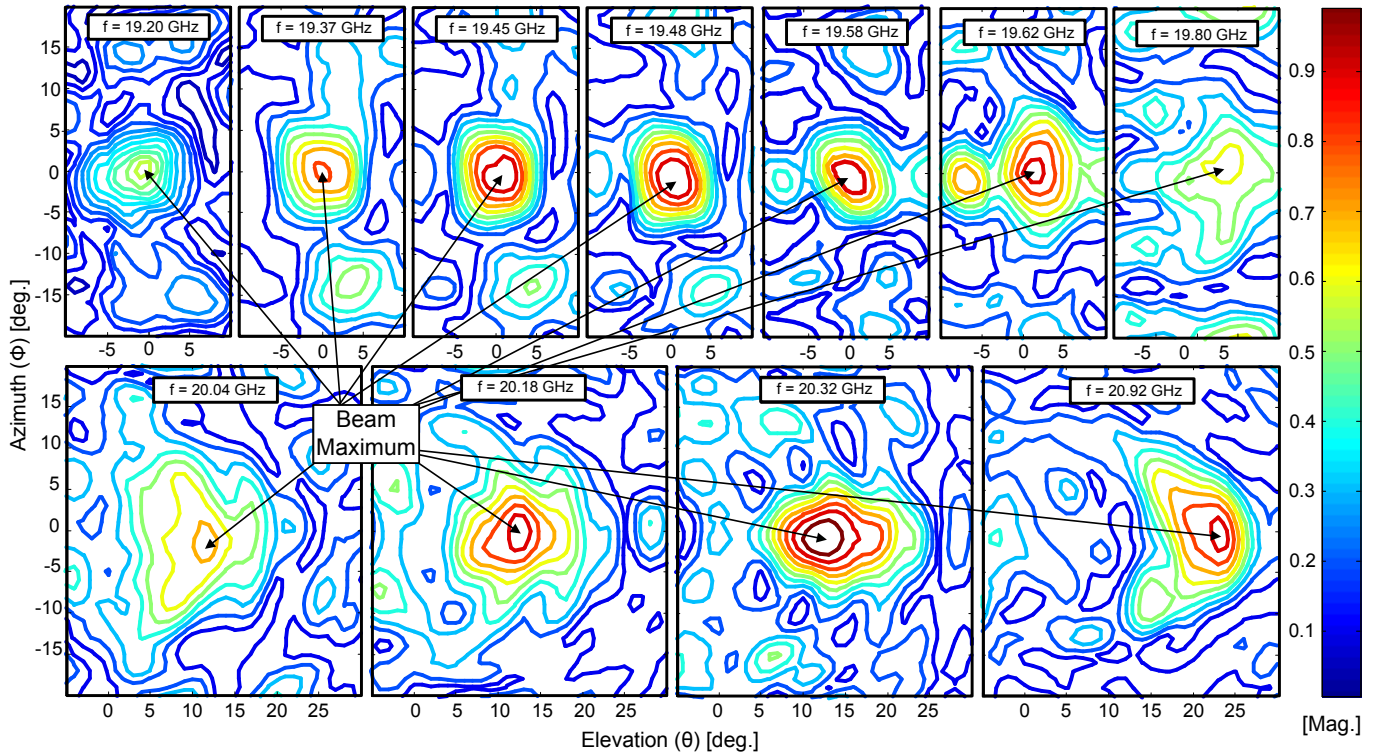


Figure 5: Measured 2D beam patterns shown in linear units and normalized to observed maximum gain at 20.32 GHz at  $\theta_p = 12.5^\circ$  GHz for Configuration I and excited by the directive-folded SWL source. Broadside pencil beams are only observed between 19.20 and 19.80 GHz while conical-sector beam scanning is achieved for  $f > 19.8$  GHz. Similar beam scanning behavior is observed for Configurations II-IV but with the noted broadside maximums (Fig. 4).

## CONCLUSION

Planar 2-D LWAs for pencil and conical-sector beam patterns were presented and discussed. By the design of a directive-folded SWL feed and an appropriately designed segmented circular strip grating configuration, both TM and TE cylindrical LWs can be efficiently excited on the antenna aperture for maximum radiation at broadside. Physically, the magnetic field distribution from the propagating SW source couples to the feedless strips defining an in phase current distribution and thus broadside radiation can be achieved. Results suggest that both TM and TE radiated components combined in the far-field achieving maximum gain at broadside near the  $TE_1$  SW mode cutoff frequency of the slab. In addition, simulations illustrate that the folded secondary slots of the SWL feed develop the prominent TE SW field distributions excited in the  $\pm y$  directions as required for increased gain values at broadside. Thus, the segmented circular strip grating, frequency of operation, substrate properties, and SWL source configuration are all central in attaining maximum gain at broadside.

## References

- [1] A. Ip and D. R. Jackson, "Radiation from Cylindrical Leaky Waves," *IEEE Trans. Antennas Propag.*, vol. 38, no. 4, pp. 482–488, Apr. 1990.
- [2] G. Lovat, P. Burghignoli, and D. R. Jackson, "Fundamental Properties and Optimization of Broadside Radiation from Uniform Leaky-Wave Antennas," *IEEE Trans. Antennas Propag.*, vol. 54, no. 5, pp. 1442–1452, May 2006.
- [3] T. Zhao, D. R. Jackson, J. T. Williams, and A. A. Oliner, "General formulas for 2-D leaky wave antennas," *IEEE Trans. Antennas Propag.*, vol. 53, no. 11, pp. 3515–3533, Nov. 2005.
- [4] S.K. Podilchak, A.P. Freundorfer, and Y.M.M. Antar, "Broadside Radiation From a Planar 2-D Leaky-Wave Antenna by Practical Surface-Wave Launching," *IEEE Antennas and Wireless Propag. Lett.*, vol. 7, pp. 516–519, 2008.
- [5] S. Mahmoud, Y.M.M. Antar, H. Hammad, and A. Freundorfer, "Theoretical Considerations in the Optimization of Surface Waves on a Planar Structure," *IEEE Trans. Antennas Propag.*, vol. 52, no. 8, pp. 2057–2063, Apr. 2004.
- [6] M. Ettore, S. Bruni, G. Gerini, A. Neto, N. Llobart, and S. Maci, "Sector PCS-EBG Antenna for Low-Cost High-Directivity Applications," *IEEE Antennas and Wireless Propagation Lett.*, vol. 6, pp. 537–539, 2007.
- [7] D. M. Pozar, D.H. Schaubert, "Scan Blindness in Infinite Phased Arrays of Printed Dipoles," *IEEE Trans. Antennas Propag.*, vol. 32, no. 6, pp. 602–610, Jun. 1984.